diversity

MDPI

Article

Leaf Senescence of the Seagrass *Cymodocea nodosa* in Cádiz Bay, Southern Spain

Rocío Jiménez-Ramos *, Carmen Henares, Luis G. Egea, Juan J. Vergara and Fernando G. Brun

Department of Biology, Faculty of Marine and Environmental Sciences, International Campus of Excellence of the Sea (CEIMAR), University of Cadiz, 11510 Puerto Real, Spain

* Correspondence: rocio.jimenez@uca.es

Abstract: Leaf decay in seagrasses is enhanced in some seasons since large green senescent beach-cast seagrass leaves are frequently recorded during autumn and winter seasons. Here, we explore if senescence is operating in seagrass leaf decay or if hydrodynamic stress is responsible for the seasonal leaf abscission. A seasonal study on the temperate seagrass *Cymodocea nodosa* was carried out in four locations with contrasting hydrodynamic regimes. The morphological, biomechanical and material properties of *C. nodosa* were measured. The force required to break the ligule was always lower than that required to break the blade. This could be considered an adaptive strategy to reduce acute drag forces and thus lessen the chance of plant uprooting. The absolute force needed to dislodge the blade at the ligule level varied with season and location, with the lowest forces recorded in autumn. This may indicate that senescence is operating in this species. On the other hand, the minimum estimated failure velocities for leaf abscission were also recorded in autumn. Consequently, this may cause the premature shedding of leaves in this season before the senescence process has finished and can probably explain the occurrence of green beach-cast seagrass leaves usually found during autumn and winter.

Keywords: leaf abscission; nutrient recycling; drag forces; biomechanics; breaking strength; seagrass; *Cymodocea nodosa*

Citation: Jiménez-Ramos, R.; Henares, C.; Egea, L.G.; Vergara, J.J.; Brun, F.G. Leaf Senescence of the Seagrass *Cymodocea nodosa* in Cádiz Bay, Southern Spain. *Diversity* **2023**, *15*, 187. https://doi.org/10.3390/d15020187

Academic Editors: Eugenia Apostolaki and Bert W. Hoeksema

Received: 19 November 2022
Revised: 18 January 2023
Accepted: 25 January 2023
Published: 29 January 2023

1. Introduction

Seagrasses form a unique ecological group of specialized flowering plants evolving from a terrestrial ancestor that returned to seawater 145 million years ago [1]. These plants are the only higher plants that carry out their whole life cycle in marine environments [2], which has led to a complex evolutionary adaptation process [3,4]. This has determined, to some extent, that most of the seagrass species share morphological, physiological and biomechanical adaptations to face marine environmental conditions (e.g., salinity, drag forces, etc.; [5–10]). Within such adaptations and to cope with the physical stress caused by water motion (waves and currents), seagrasses display a reduced exposed surface and a flexible above-ground biomass allowing reconfiguration of the canopy to minimize drag forces [10–12]. This simple architectural design means that in most species, leaf loss often takes place at the point of junction between the blade and the leaf sheath in the oldest leaf (i.e., at the ligule; [11,12]), as occurs in terrestrial plants during senescence [13]. In addition, this above-ground biomass (i.e., leaves clustered in shoots) is attached to a well-developed below-ground biomass (i.e., rhizomes and roots), keeping plants firmly secured to the sediment.

Senescence is a fundamental developmental step in the life cycle of annual and perennial plants and is considered a type of programmed cell death [14–17]. During senescence, a set of highly regulated processes at different organizational levels (i.e., molecular, biochemical, physiological) is triggered, which allows the controlled remobilization of nutrients from old to young tissues or to the development of fruits or seeds [18–22]. Senescence is clearly

distinguished in deciduous plants by the decolourisation of the leaves in autumn and their concomitant abscission and decay, while in annual ones, the final stage usually means the death of the whole plant [17,22,23]. Therefore, although leaf senescence may follow similar stages and biochemical pathways, the meaning of such a mechanism is different in both types of plants [24–27]. Similar to other physiological processes in plants, leaf senescence is regulated by endogenous and exogenous factors: photoperiod, temperature, shading, nutrient deficiency, drought, internal sugar concentrations and hormone levels, among others [28–31]. While the evolutionary importance and molecular mechanisms underlying senescence have been extensively studied in terrestrial plants, including annual and perennial ones [19,20,32], little is known in the case of marine plants.

As happens in terrestrial plants [33], leaf decay in seagrasses is enhanced during some seasons (i.e., autumn and winter) [34–38], and it can also be triggered as a response to exogenous signals such as nutrient deficiency or excess [39–41], light levels [42–44], flow velocity [45] and organic matter in the sediment [46], among others. However, during leaf decay, remobilization of nutrients from shedding leaves is limited in comparison with terrestrial plants [36,47–50], which is referred to as the "nutrient paradox" theory in seagrasses [51]. The recycling of nutrients from decayed leaves in seagrasses ranged from 3.8% to 64% in the case of nitrogen and from 0% to 64% in the case of phosphorus [35,50,52,53], indicating a lower capacity of nutrient recycling in comparison to terrestrial plants, where recycling was reported to reach 79% for N and 90% for P [32,54–57]. In contrast to terrestrial plants, where senescence leads to the remobilization of the main nutrients from leaves, senescent beach-cast seagrass leaves during autumn and winter are usually still green and have a high proportion of the main nutrients [58–63].

Following the aforementioned arguments, the question arises about whether seasonal senescence operates in seagrasses or, conversely, hydrodynamic stress is responsible for the seasonal leaf fall. We hypothesized that if seasonal senescence operates in seagrasses, leaf abscission, the last step in this highly regulated process, may have a seasonal variation, which can be estimated through material mechanical failure at the ligule level [63]. In contrast, the lack of seasonality would indicate that leaf loss is promoted by hydrodynamic conditions, causing a sudden interruption of senescence and consequently of nutrient recycling. Therefore, the aim of this work was to identify whether seasonal senescence or hydrodynamic stress is the main factor responsible for seasonal leaf fall in the temperate seagrass *Cymodocea nodosa* in Cádiz Bay, southern Spain. To ascertain the role of leaf senescence and hydrodynamic stress, biomechanical properties (the force needed to separate the blade from the sheath), leaf morphology and material properties were measured seasonally at different locations covering a large hydrodynamic range.

2. Material and Methods

2.1. Sampling Locations and Biological Material

Cádiz Bay (south of Spain; Figure 1) follows the typical seasonality of temperate climates, with maximum values for temperature and light during summer and storm periods in winter [64,65]. The mesotidal and semidiurnal tidal regime has a mean range of 2.3 m and a mean spring tidal range of 3.7 m [66]. Waves generally approach the coast from the west and south, giving rise to a prevailing East and Southeast longshore current [66].

Figure 1. Map of the study area in Cádiz Bay (SW Spain) showing dominant seagrass distribution and experimental locations where *Cymodocea nodosa* shoots were collected. Locations (from high to low exposure): CH, El Chato (high exposure to waves, intertidal); BC, Bajo de la Cabezuela (medium exposure to waves and currents, subtidal); ST, Santibáñez (low exposure to waves and currents) with two stations: intertidal (ST-Int) and subtidal (ST-Sub); CC, Caño de Cortadura (no waves, low exposure to currents).

Seagrass zonation with increasing elevation in Cádiz Bay includes extensive meadows of *Cymodocea nodosa*, with meadows of the seagrass *Zostera noltei* Hornem. in the lower intertidal area [67]. The temperate seagrass species *Cymodocea nodosa* Ucria (Ascherson) was selected because it forms perennial populations and inhabits locations with different environmental conditions in Cádiz Bay: Caño de Cortadura (CC), Santibáñez (ST), El Bajo de la Cabezuela (BC), El Chato (CH) (Figure 1, Table 1). *C. nodosa* is the unique seagrass species inhabiting areas of contrasting hydrodynamics in Cádiz Bay, from very high to very low hydrodynamics, while *Z. noltei* is currently restricted to sheltered areas of low hydrodynamics.

Table 1. Summary of the environmental conditions at each experimental location.

	CC	ST	BC	CH
Latitude	36°52′60′′ N	36°28′09.08′′ N	36°31′42.52′′ N	36°28′38.16′′ N
Longitude	6°21′77′′	6°15′04.64′′ W	06°14′32.16″ W	06°15′49.21′′ W
Depth (m)	0.25	0.5	0.5	0.25
Hydrodynamic exposure	Very low	Low	Medium	High
Experimental meadow area (ha)	0.36	0.8	0.77	0.74

The Caño de Cortadura (CC) is a small and shallow lagoon (≈0.73 ha and 1.5 m maximum depth) located near the San Pedro River and connected to the river through a small artificial channel. This artificial opening ensures that this area is subject to very low levels of hydrodynamic forces, that is, without waves and influenced only by semidiurnal tidal oscillations. *C. nodosa* develops in continuous and homogeneous meadows

covering approximately 50% of the lagoon area with a mean annual shoot density of 250 ± 50 shoots m^{-2} [66]. Santibáñez saltmarsh (ST), located at the southern point of the inner sector of Cádiz Bay, is a shallow tidal lagoon. This is a site of low hydrodynamics with little exposure to waves. The mean velocity module during a usual tidal cycle ranges from 0.015 to 0.08 m s^{-1} [68,69], which increases when strong eastern winds blow and during winter [70]. *C. nodosa* inhabits the shallow south-western area at both the intertidal fringe (ST-Int) and as continuous monospecific meadows in the subtidal zone (ST-Sub), at 0.4 and −0.5 m above and below the chart datum (lowest astronomical tide) [67]. *C. nodosa* populations at Santibáñez exhibit a unimodal seasonal pattern of growth, with maximum growth rates and shoot sizes in summer [71–73]. The shoot density and biomass in this area vary with tidal position, with mean annual values of 1194 ± 513 and 447 ± 174 shoots m^{-2}, respectively, in the intertidal and subtidal areas [67,74]. The Bajo de la Cabezuela (BC) is a shallow inlet located in the Rio San Pedro saltmarsh. Continuous beds of *C. nodosa* colonize the shallow sandy subtidal zones, with an average shoot density of 154 ± 32.7 shoots m^{-2} [66]. Plants were collected at the mouth of the inlet, a location subjected to high currents powered by tide, short-periods of wind-generated waves (which increased during winter) and recurrent episodes of sediment erosion and accretion [70]. The mean velocity module measured during a tidal cycle ranged from 0.05 to 0.25 m s^{-1} [68]. El Chato (CH) is a shoreline-parallel rocky outcrop located at Cortadura beach, facing the open ocean with a NNW–SSE orientation [75]. The hydrodynamic conditions of this location differ highly from those at the other locations, as it is the only location exposed to open ocean and thus strong currents (data not available) and large waves. *C. nodosa* forms small scattered patches in the rocky pools with a mean annual density of 95 ± 17 shoots m^{-2} [66].

These four locations were selected since one of the most noticeable abiotic factors differentiating the locations was the hydrodynamic regime, as they have contrasting exposure to waves and currents (Table 1). As a consequence, all of these populations are acclimatized to such contrasting mechanical forces [73], allowing us to check the existence of seasonality in the force needed to separate the blade and the sheath across a wide range of morphological and biomechanical traits.

Sampling was done seasonally (four times during 2016; winter, end of January; spring, end of April; summer, end of August; autumn, end of October; and winter, end of January 2017) in the middle of each season at each location. During each sampling event, plants were randomly collected at low tide, digging a 15 × 15 cm metal square into the sediment, extracting the plants by hand and placing them in individual mesh bags. Collected plants were formed by several shoots joined by a piece of horizontal rhizome. The procedure was repeated at least 20 times in each location, attempting to leave a gap of ten metres between collected samples. Plants were first cleaned in the field and transported under cold conditions to the laboratory in darkness within two hours and placed in an illuminated aquarium with aerated natural seawater until measurements were conducted. All measurements were done within two days of collection.

2.2. Leaf Morphology

Shoots were carefully selected from the collected material, discarding those with flawed or nicked leaves, which would result in misjudgement of their mechanical properties. Epiphytes were also removed carefully from the leaf using a piece of soft-wet paper. Selected shoots were submerged into seawater at room temperature (20 °C) until testing was conducted.

All morphometric measures were taken 1 cm above the ligule of the oldest leaf of the shoot (the outermost leaf) before mechanical tests were performed [73]. Total leaf length (LL, cm), leaf width (LW, mm) and thickness (LTh, mm) were measured with a digital caliper (Mitutoyo 500 AOS) and a thickness gauge (Mitutoyo 7301). The cross-sectional area was calculated (CA, mm^2; CA = LW · LTh) [76]. The one-sided surface area of each leaf (SA, mm^2) was approximated to a rectangular shape (SA = LW · LL)[76]. In total,

10 samples (n = 10), coming from independent shoots, were measured at each location and in each season.

2.3. Leaf Internal Composition

For each tissue analysis, a minimum of 5 independent replicates were used per location and season. Samples were freeze-dried and ground in a ball-grinder, and the fibre content (i.e., NDF = neutral detergent fibre) in the leaves was measured using the method of Van Soest et al. (1991) [77] as amended by de los Santos et al. (2013) [73]. Total carbon and nitrogen contents were determined on freeze-dried, ground samples of leaves and roots/rhizomes using the PerkinElmer® 2400 Series CHNS/O Elemental Analyzer (Cádiz, Spain).

2.4. Leaf Biomechanical Measurements

The tensile properties of the leaves were measured on the oldest one (i.e., first outermost leaf) with a tensometer (Instron universal testing machine model 3340) and Bluehill software (version 2.18; BlueHill® Instron Universal, Barcelona, Spain), using a load cell of 100 N and pneumatic action grips of 250 N (model 2712). Intact leaves were clamped (approximately 4 cm above and below the ligule) with the exact distance measured to the closest 1 mm. Once clamped into the grips, the leaf was stretched at a constant velocity of 10 mm min^{-1}, while the displacement (mm) and the force (F, N) were recorded every 0.1 s until breakage, when the maximum force (absolute force-to-tear, F_{TA}, N) was registered. The tensile properties were recorded when the leaf broke, while those specimens that slipped during the test or broke at the grips were excluded from the analysis (less than 5%). In addition, another 10 independent leaves from each sampling event were selected, and the blade was cut at 1 cm above the ligule. Then, a portion of a blade of 5 cm measured from the already cut end was clamped into the grips, and the tensile properties were measured as aforementioned. From the force–displacement curve and the morphological traits of the specimens, the following mechanical properties were obtained: (a) the absolute force-to-tear (FTA, N), which is the maximum force that the specimen can bear before breaking, and (b) the specific force-to-tear (FTS, N mm^{-2}), which is the maximum force per unit of cross-sectional area needed to break the specimen. The latter is also known as 'tensile strength' or 'breaking stress' in engineering [78].

The ratio between the blade and ligule F_{TA} values (i.e., F_{TA} Blade · (F_{TA} Ligule)$^{-1}$ · 100) was calculated to examine whether the leaf was more likely to broke at the blade (values lower than 100%) or at the ligule (values higher than 100%). Coefficients of variation (i.e., CV, %) for F_{TA} and F_{TS} were also calculated for the blade and the ligule for different seasons and locations.

2.5. Predicting Failure Velocity

The theoretical flow velocity causing tissue breakage was calculated using the following drag force expression [79,80]:

$$F_d = 0.5 \cdot \rho \cdot u^2 \cdot S_A \cdot C_d \quad (1)$$

where F_d is the drag force (N), ρ is the seawater density (Kg m^{-3}), u is the water velocity (m s^{-1}), S_A is the one-side surface area of the leaf (i.e., planform area, in m^2) and C_d is the drag coefficient, a dimensionless index of shape change and reconfiguration of flexible fronds. Therefore, once having measured the absolute force-to-tear at the ligule (F_{TA} ligule, N) at the different locations and in different seasons, the aforementioned equation was solved for the water flow (u) required to generate such a breakage force. A value of 1025 Kg m^{-3} was used for seawater density. Experimental drag coefficients calculated by Kopp (1999) [38] in the temperate seagrass *Zostera marina* at high Reynolds numbers (300,000) were used in our calculations. Estimated drag coefficients for both large and small size-class shoots and individual and whole shoots (see Table 6 from [38]) were used to estimate a range of failure velocities for each F_{TA} ligule value.

2.6. Statistical Analysis

The effect of location on leaf morphometry (length, width, thickness and cross-sectional area), internal composition (NDF, %N, %C and C/N ratio) and leaf-breaking force (F_{TA} and F_{TS} at blade and ligule) was examined using a linear mixed-effects regression model. Location was included as a fixed factor (4 levels of hydrodynamic conditions) with season as a random factor in order to investigate how much of the variation in leaf properties was attributable to the season. The model was fitted for maximum likelihood, and Type II Wald χ^2 tests were used to assess the significance of the fixed effect in the model. Pairwise comparisons to identify homogenous groups were identified using Tukey's multiple comparison tests. Significance was considered at $p < 0.05$. Data were also visualized and tested for correlations (Pearson correlations) between each pair of variables (leaf morphology, internal composition and biomechanics) through the 'corrplot' R library [81].

To analyse the influence of leaf morphometry (length, width, thickness and cross-sectional area) and the internal composition variables (NDF, %N, %C and C/N ratio) on the biomechanical variables (F_{TA} and F_{TS} at the ligule and blade), generalized linear models (GLMs) were performed. Gaussian distributions with an "identity" link function were selected to ensure the assumptions of linearity and homogeneity of variances, which were checked through visual inspection of residuals and Q–sQ plots [82]. Variable collinearity was analysed through Variation Inflation Factor (VIF) of preliminary full GLMs. Cross-correlated and non-informative variables were removed from GLMs using backward selection to retain only those predictor variables associated with the response variables. We calculated models with all possible combinations of predictor variables using the MuMIn package [83] and selected the best fit model using Akaike's Information Criterion (AIC). Finally, we used generalized linear models (GLMs) to quantify how the predictor variables from the best-fit model interacted with the response variables. Data are shown as means ± standard error. Statistical analyses were computed with R statistical software version 4.0.2 (R Foundation for Statistical Computing, Vienna, Austria) [84].

3. Results

3.1. Morphological and Internal Composition

Shorter leaves were more common in most of the locations in winter, while longer ones were common during summer–autumn, regardless of the location in the bay (Figure 2A; Table 2). Seagrass in the high exposure (CH) area had the shortest leaves throughout the year (6.6 ± 1.6 cm), while seagrass in the subtidal area (ST) had the longest ones (35.4 ± 6.3 cm; linear mixed-effects model, degrees of freedom (df) = 1, $p = 0.019$, $\chi^2 = 6.74$; Table 2). Leaf width and thickness also showed seasonal, but opposite trends. While thicker leaves were usually recorded in winter and thinner leaves in summer, wider leaves were found in summer–autumn, with minimum thickness values in winter (Figure 2B,C; Table 2). Thicker leaves were those coming from subtidal populations, independently of hydrodynamic conditions (0.37 ± 0.03, 0.36 ± 0.03 and 0.29 ± 0.01 mm for BC, ST-Sub and CC, respectively), while those inhabiting intertidal areas had lower values (0.24 ± 0.03 and 0.26 ± 0.03 mm in CH and ST-Int, respectively; linear mixed-effects model, df = 1, $p < 0.017$, $\chi^2 = 6.23$; Table 2). Plants inhabiting exposed areas had lower width values (2.66 ± 0.26 and 3.4 ± 0.43 mm for CH and BC, respectively), while subtidal populations inhabiting areas with low exposure were wider (4.4 ± 0.36 and 4.0 ± 0.35 mm for ST-Sub and CC, respectively). The surface area showed a seasonal trend, with minimum values in winter (5.4 ± 1.88 cm^2), which increased from spring and reached maximum values in autumn (14.7 ± 1.82 cm^2) (Figure 3A; Table 2; linear mixed-effects model, df = 1, $p < 0.012$, $\chi^2 = 5.19$). Exposed populations from CH bore the lowest surface areas (1.9 ± 0.6 cm^2), which were almost ten times lower than those values registered for the ST-Sub populations (16.7 ± 4.2 cm^2) (Figure 3A; Table 2). Plants from exposed and intertidal areas (CH and ST-Int) displayed the lowest cross-sectional area (CA, 0.63 ± 0.07 mm^{-2} and 0.98 ± 0.13 mm^{-2}), while plants from subtidal areas had the highest values (i.e., ST-Sub, 1.57 ± 0.19 mm^{-2}; Figure 3B; Table 2). Seasonality was not as clear as S_A, but most

of the locations had CA values that increased until autumn and decreased in winter (Figure 3B; Table 2).

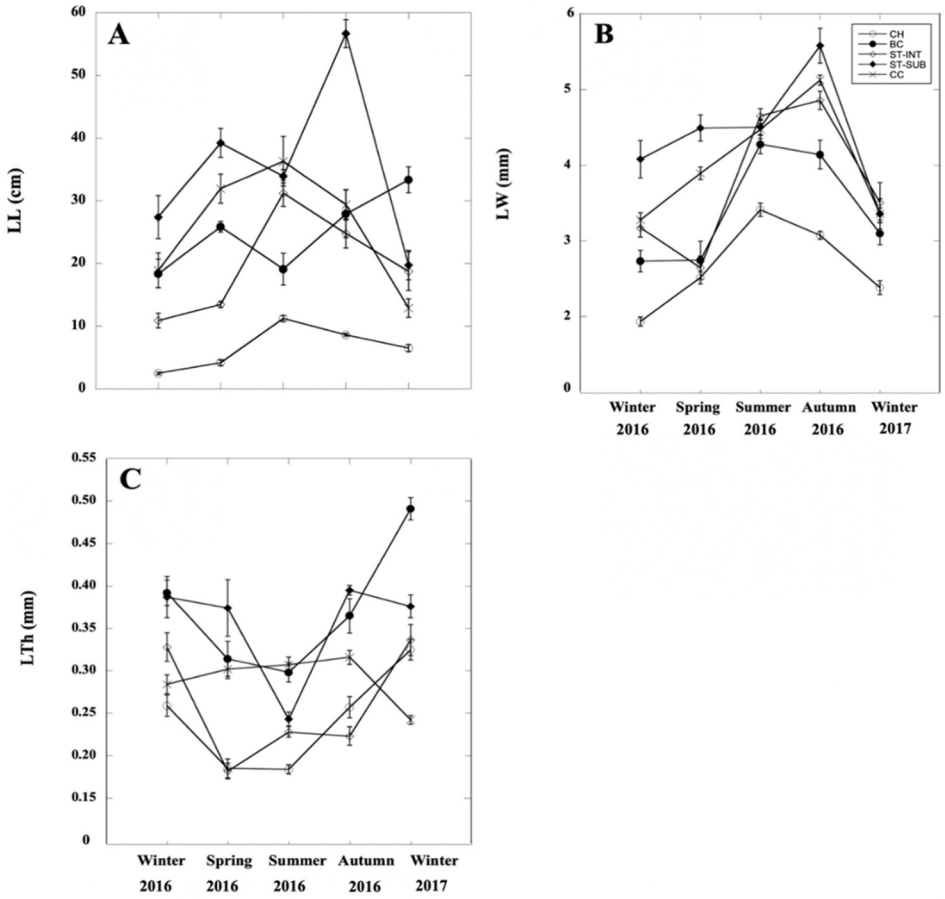

Figure 2. Seasonal variation of the morphological leaf traits of *Cymodocea nodosa*. (**A**) Leaf length (LL); (**B**) Leaf width (LW); (**C**) Leaf thickness (LTh). Values are presented as the mean ± SE (n = 10). Locations (from high to low exposure): CH, El Chato (high exposure to waves, intertidal); BC, Bajo de la Cabezuela (medium exposure to waves and currents, subtidal); ST, Santibáñez (low exposure to waves and currents) with two stations: intertidal (ST-Int) and subtidal (ST-Sub); CC, Caño de Cortadura (no waves, low exposure to currents).

The leaf internal composition differed between locations and seasons (Table 2). Internal carbon and nitrogen contents followed a similar seasonal trend with lower values in summer–autumn and maxima in winter at all locations (Figure 4A,B; Table 2). The C/N ratios remained rather stable across locations with a clear seasonal trend with maximum values in autumn (Figure 4C; Table 2). The fibre content (NDF) showed a significant seasonal trend with higher values in summer–autumn and minimum ones in winter-spring depending on the location, although location had no effect on the fibre content (Figure 4C; Table 2).

Table 2. Summary of the morphometric, internal composition and mechanical properties of *Cymodocea nodosa* leaves in different locations and seasons (mean ± SE, n = 5). Statistical results of a linear mixed-effects model, with location as a fixed factor and season as a random factor, are presented. Superscript letters represent post hoc Tukey pairwise groupings indicating differences between locations. F_{TA}Blade: absolute force to tear the blade; F_{TA}Ligule: absolute force-to-tear at the ligule; F_{TS}Blade: specific force to tear the blade; F_{TS}Ligule: specific force-to-tear at the ligule; F_{TA}Blade/F_{TS}Ligule: ratio of the specific force to tear the blade/specific force-to-tear at the ligule. Locations (from high to low exposure): CH, El Chato (high exposure to waves, intertidal); BC, Bajo de la Cabezuela (medium exposure to waves and currents, subtidal); ST, Santibáñez (low exposure to waves and currents) with two stations: intertidal (ST-Int) and subtidal (ST-Sub); CC, Caño de Cortadura (no waves, low exposure to currents). *p*-values in bold indicate significant differences.

Leaf Traits			**Location**			**Linear Model Effect (df = 1)**	
	CH	BC	ST-Int	ST-Sub	CC	χ^2	*p*-value
Leaf Length (cm)	6.59 ±1.55	24.9 ± 2.81	19.8 ± 3.71	35.4 ± 6.25	25.9 ± 4.34	6.74	**0.019**
Leaf Width (mm)	2.66 ± 0.26	3.40 ± 0.34	3.77 ± 0.43	4.40 ± 0.36	4.03 ± 0.35	5.22	**0.03**
Leaf Thickness (mm)	0.24 ± 0.03	0.37 ± 0.03	0.26 ± 0.03	0.36 ± 0.03	0.29 ± 0.01	6.23	**0.017**
Surface area (cm^2)	1.92 ± 0.60	8.56 ± 1.18	8.04 ± 2.24	16.7 ± 4.20	10.9 ± 2.41	7.23	**0.007**
Cross-sectional area (mm^2)	0.63 ± 0.07	1.24 ± 0.13	0.98 ± 0.13	1.57 ± 0.19	1.18 ± 0.15	4.23	**0.009**
Fibre content (% DW)	38.5 ± 1.51	38.7 ± 2.41	41.0 ± 2.27	35.6 ± 2.48	36.5 ± 1.95	0.06	0.43
%C	31.5 ± 1.26	31.1 ± 0.68	33.2 ± 0.36	33.0 ± 0.29	31.6 ± 1.69	3.76	**0.042**
%N	2.63 ± 0.13	2.42 ± 0.14	2.73 ± 0.15	2.70 ± 0.06	2.64 ± 0.30	2.64	**0.037**
C/N	14.0 ± 0.20	15.2 ± 0.63	14.4 ± 0.64	14.4 ± 0.24	14.4 ± 0.92	2.97	**0.04**
F_{TA} Blade (N)	2.85 ± 0.24	5.85 ± 0.78	3.33 ± 0.39	5.36 ± 0.50	3.79 ± 0.34	5.12	**0.022**
F_{TA} Ligule (N)	2.39 ± 0.18	3.47 ± 0.60	2.72 ± 0.66	3.64 ± 0.39	2.39 ± 0.05	4.82	**0.013**
F_{TS} Blade ($N{\cdot}mm^{-2}$)	4.70 ± 0.32	4.97 ± 0.55	3.57 ± 0.21	3.83 ± 0.67	3.44 ± 0.58	3.65	**0.036**
F_{TS} Ligule ($N{\cdot}mm^{-2}$)	4.10 ± 0.61	2.87 ± 0.43	2.83 ± 0.47	2.52 ± 0.40	2.12 ± 0.24	3.12	**0.041**
F_{TA} Blade/F_{TA} Ligule (%)	133 ± 10.5	185 ± 14.5	164 ± 35.4	164 ± 11.3	187 ± 27.8	4.23	**0.02**
Leaf Traits			Season			Linear model effect (df = 1)	
	Winter	Spring	Summer	Autumn	Winter	χ^2	*p*-value
Leaf Length (cm)	15.6 ± 4.4	22.9 ± 3.94	26.3 ± 4.42	29.5 ± 4.26	18.2 ± 5.91	2.93	**0.017**
Leaf Width (mm)	3.04 ± 0.35	3.26 ± 0.27	4.26 ± 0.27	4.56 ± 0.29	3.14 ± 0.36	1.64	**0.034**
Leaf Thickness (mm)	0.33 ± 0.03	0.27 ± 0.04	0.25 ± 0.03	0.31 ± 0.04	0.35 ± 0.04	2.94	**0.027**
Surface area (cm^2)	5.43 ± 1.88	8.32 ± 1.81	11.6 ± 1.83	14.7 ± 1.82	6.01 ± 2.79	5.19	**0.012**
Cross-sectional area (mm^2)	1.03 ± 0.18	0.93 ± 0.18	1.09 ± 0.18	1.44 ± 0.21	1.12 ± 0.21	3.84	**0.03**
Fibre content (% DW)	36.0 ± 1.97	34.6 ± 1.39	40.6 ± 1.37	43.9 ± 0.66	35.2 ± 0.47	1.64	**0.041**
%C	33.7 ± 0.38	31.3 ± 1.15	30.0 ± 1.25	31.5 ± 1.21	33.9 ± 1.22	4.26	**0.036**
%N	2.97 ± 0.12	2.50 ± 0.17	2.36 ± 0.2	2.34 ± 0.18	2.95 ± 0.18	7.13	**0.016**
C/N	13.3 ± 0.39	14.7 ± 0.42	14.9 ± 0.49	15.9 ± 0.47	13.5 ± 0.48	6.95	**0.011**
F_{TA} Blade (N)	4.52 ± 0.57	3.64 ± 0.68	4.04 ± 0.69	4.05 ± 0.89	4.93 ± 0.81	6.42	**0.015**
F_{TA} Ligule (N)	3.39 ± 0.50	2.38 ± 0.58	2.90 ± 0.53	2.24 ± 0.65	3.70 ± 0.39	4.26	**0.01**
F_{TS} Blade ($N{\cdot}mm^{-2}$)	4.70 ± 0.38	4.40 ± 0.31	3.84 ± 0.49	3.26 ± 0.42	4.31 ± 0.48	4.85	**0.013**
F_{TS} Ligule ($N{\cdot}mm^{-2}$)	3.64 ± 0.74	2.99 ± 0.60	2.86 ± 0.19	1.74 ± 0.26	3.21 ± 0.44	3.85	**0.02**
F_{TA} Blade/F_{TA} Ligule (%)	149 ± 22.3	153 ± 23.2	141 ± 12.4	203 ± 8.8	159 ± 28.6	5.24	**0.036**

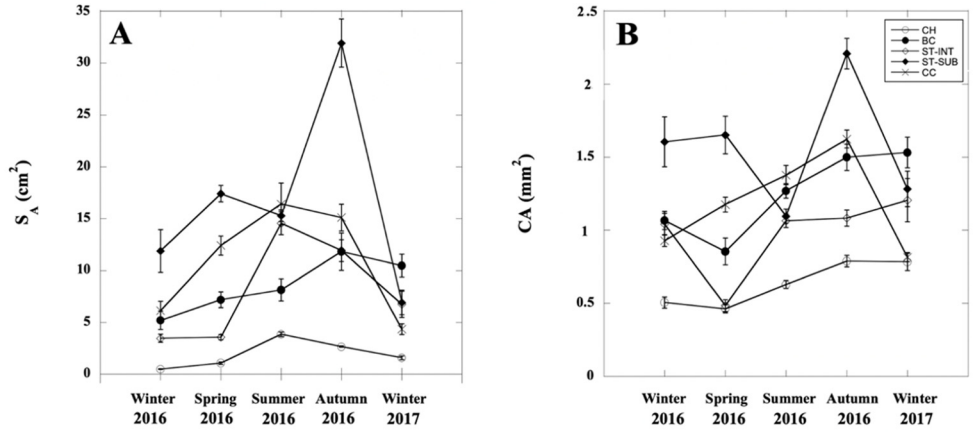

Figure 3. Seasonal variation of (**A**) Surface area (S_A) and (**B**) Cross-sectional area (CA) in *Cymodocea nodosa*. Values are presented as the mean ± SE (n = 10). Locations (from high to low exposure): CH, El Chato (high exposure to waves, intertidal); BC, Bajo de la Cabezuela (medium exposure to waves and currents, subtidal); ST, Santibáñez (low exposure to waves and currents) with two stations: intertidal (ST-Int) and subtidal (ST-Sub); CC, Caño de Cortadura (no waves, low exposure to currents).

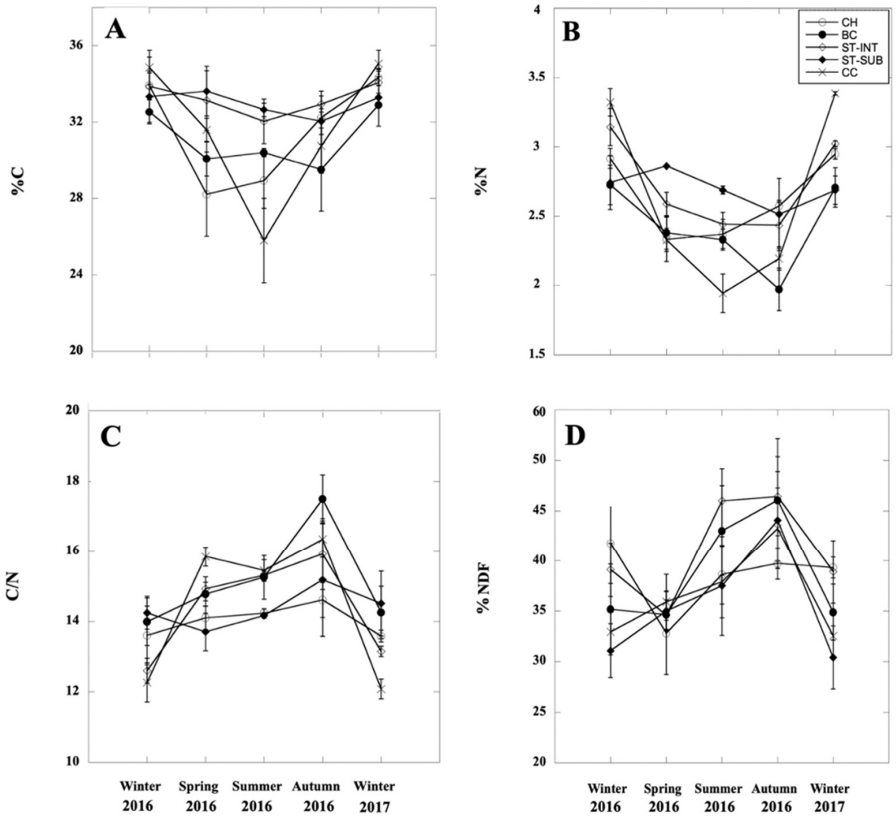

Figure 4. Internal composition of *Cymodocea nodosa* leaves in different locations and seasons. (**A**) Internal carbon content (%C); (**B**) Internal nitrogen content (%N); (**C**) Carbon/nitrogen ratio (C/N); (**D**) Fibre content (%NDF). Values are presented as the mean ± SE (n = 5). Locations (from high to low exposure): CH, El Chato (high exposure to waves, intertidal); BC, Bajo de la Cabezuela (medium exposure to waves and currents, subtidal); ST, Santibáñez (low exposure to waves and currents) with two stations: intertidal (ST-Int) and subtidal (ST-Sub); CC, Caño de Cortadura (no waves, low exposure to currents).

3.2. Biomechanical Properties

All assayed leaves broke at the ligule (95%) during the biomechanical measurements, while only a few specimens slipped or broke at the grip (<5%). Both absolute (F_{TA}) and specific forces (F_{TS}) were repeatedly higher in blades than at the ligule, indicating that it was easier to split the leaf at the ligule rather than at the blade (Figure 5; Table 2). Overall, winter was the season where leaves had higher values of F_{TA} for both the blade and ligule, while lower values were recorded in spring and autumn (Figure 5A,B; Table 2). Lower absolute forces needed to tear the blade and the ligule were recorded in areas with high hydrodynamics and small plants (CH), while higher values were recorded in areas with high currents and long plants (BC and ST-Sub), but also in areas of low current and long plants (e.g., CC) (Figure 5A,B; Table 2). It was noticeable that in CC (very low hydrodynamic conditions), the absolute force needed to tear the ligule remained constant across all seasons (Figure 5B).

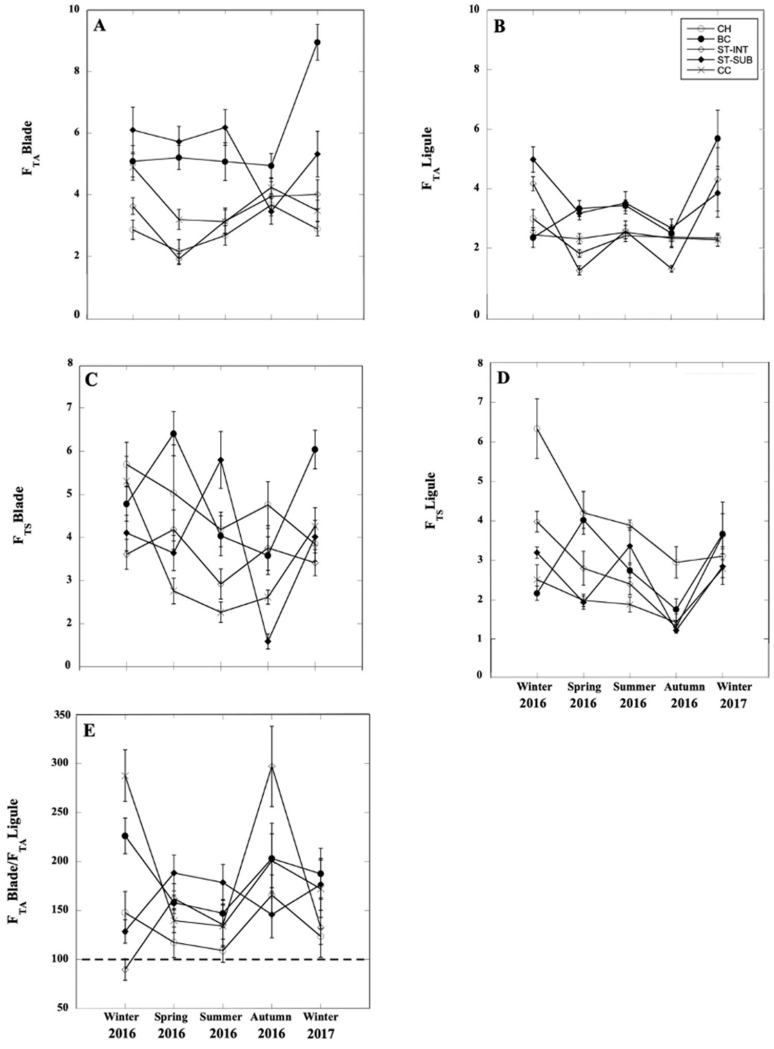

Figure 5. Biomechanical traits in *Cymodocea nodosa* leaves in different locations and seasons. (**A**) Absolute force to tear the blade (F_{TA}Blade); (**B**) Absolute force-to-tear at the ligule (F_{TA}Ligule); (**C**) Specific force to tear the blade (F_{TS}Blade); (**D**) Specific force-to-tear at the ligule (F_{TS}Ligule); (**E**) Ratio of the specific force to tear the blade/specific force-to-tear at the ligule (F_{TA}Blade/F_{TS}Ligule). Values are presented as the mean ± SE (n = 10). Locations (from high to low exposure): CH, El Chato (high exposure to waves, intertidal); BC, Bajo de la Cabezuela (medium exposure to waves and currents, subtidal); ST, Santibáñez (low exposure to waves and currents) with two stations: intertidal (ST-Int) and subtidal (ST-Sub); CC, Caño de Cortadura (no waves, low exposure to currents).

When material size was considered (i.e., F_{TS}), it reduced the seasonal variability at each location, and a clear trend was observed in most of the locations for the blade and ligule, with minimum values in autumn and maximum values in winter (Figure 5C,D; Table 2). Plants from exposed areas had, on average, higher F_{TS} values (CH and BC) when compared to plants inhabiting low-exposure, more protected areas (ST-Int, ST-Sub and CC) (Figure 5C,D; Table 2). Both F_{TA} and F_{TS} were significantly correlated with CA (Figure 6).

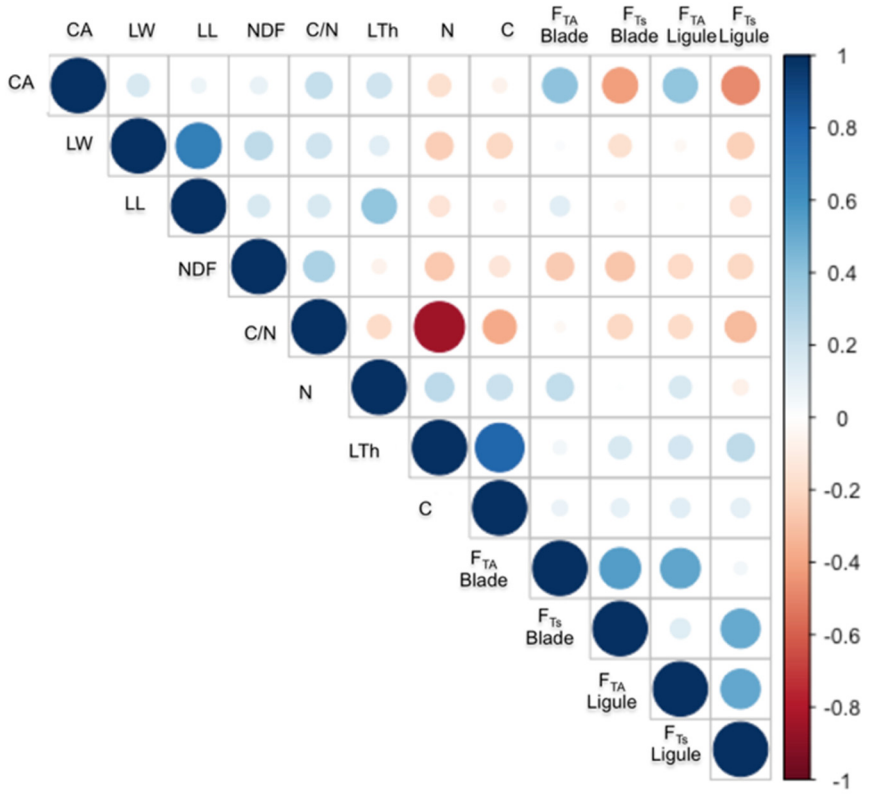

Figure 6. Pairwise Pearson's correlation coefficient between leaf properties. Correlations were performed between average values for each location. Points are coloured and sized according to the value of the Pearson's correlation coefficient.

The F_{TA} Blade/F_{TA} Ligule ratio showed slight variability throughout the year and between locations, with the highest value recorded in autumn (203 ± 8.8%; linear mixed-effects model, df = 1, p = 0.036, χ^2 = 5.24) and the minimum value found in the most exposed area (132 ± 10.1%) (Figure 5; linear mixed-effects model, df = 1, p = 0.02, χ^2 = 6.23; Table 2). Coefficients of variation for F_{TA} and F_{TS} for the blade and ligule were rather similar throughout the year and between locations, with values raging from 20 to 50%, although most of them were around 30% (Table 3).

3.3. Generalized Linear Model Analyses

After the removal of the collinear and non-informative variables, fitted GLMs included the leaf length, width and thickness, fibre content and C/N ratios as predictors of F_{TA} and F_{TS} at the ligule and blade (Table 4). The most parsimonious model explaining F_{TA} at the ligule included leaf thickness and the C/N ratio, whereas the most parsimonious model to explain F_{TA} at the blade included the leaf length and thickness. F_{TA} at both the ligule and blade was positively and significantly associated with leaf thickness (Table 4). The most parsimonious model explaining F_{TS} at the ligule included leaf width and the C/N ratio, whereas the most parsimonious model explaining F_{TS} at the blade included the leaf length, width and fibre content (Table 4). F_{TS} at the ligule was negatively associated with leaf width, whereas F_{TS} at the blade was negatively associated with leaf width and was positively associated with leaf length and fibre content (Table 4).

Table 3. Coefficient of variation (%) of biomechanical traits measured in *Cymodocea nodosa* leaves in different locations and seasons (mean ± SE, n = 5). F_{TA}Blade: absolute force to tear the blade; F_{TA}Ligule: absolute force-to-tear at the ligule; F_{TS}Blade: specific force to tear the blade; F_{TS}Ligule: specific force-to-tear at the ligule. Locations (from high to low exposure): CH, El Chato (high exposure to waves, intertidal); BC, Bajo de la Cabezuela (medium exposure to waves and currents, subtidal); ST, Santibáñez (low exposure to waves and currents) with two stations: intertidal (ST-Int) and subtidal (ST-Sub); CC, Caño de Cortadura (no waves, low exposure to currents). *p*-values in bold indicate significant differences.

Coefficient of Variation (CV)			**Location**			**Linear model effect (df = 1)**	
	CH	BC	ST-Int	ST-Sub	CC	χ^2	*p*-value
F_{TA} Blade (%)	37.15 ± 5.34	27.29 ± 3.29	33.29 ± 3.73	34.30 ± 2.52	29.30 ± 2.92	3.41	**0.023**
F_{TA} Ligule (%)	25.65 ± 5.99	34.69 ± 6.43	38.39 ± 9.11	36.59 ± 7.93	27.25 ± 4.35	4.16	**0.034**
F_{TS} Blade (%)	39.45 ± 7.75	29.25 ± 2.65	33.87 ± 3.27	32.59 ± 1.52	29.70 ± 2.73	3.72	**0.01**
F_{TS} Ligule (%)	28.28 ± 5.70	30.74 ± 5.98	39.82 ± 7.94	34.38 ± 6.41	28.43 ± 4.55	1.06	0.38
Coefficient of Variation (CV)			Season			Linear model effect (df = 1)	
	Winter	Spring	Summer	Autumn	Winter	χ^2	*p*-value
F_{TA} Blade CV (%)	30.06 ± 2.62	33.91 ± 6.07	37.60 ± 6.43	29.97 ± 5.97	29.80 ± 6.09	0.23	0.42
F_{TA} Ligule CV (%)	28.54 ± 5.96	26.11 ± 5.32	26.42 ± 2.38	35.10 ± 3.84	46.39 ± 3.91	3.56	**0.013**
F_{TS} Blade CV (%)	29.20 ± 1.02	39.88 ± 8.18	34.86 ± 8.26	33.29 ± 8.05	27.62 ± 7.83	4.53	**0.037**
F_{TS} Ligule CV (%)	20.72 ± 2.50	31.15 ± 4.73	28.26 ± 4.85	40.01 ± 7.11	41.50 ± 6.38	3.98	**0.023**

Table 4. Results of the GLM analysis showing the effects and significance of the leaf internal composition (fibre content and C/N ratio) and leaf morphometry (width, thickness, length) variables on the biomechanical variables (F_{TA} and F_{TS} at the blade and ligule). Significant predictors for each biomechanical variable are highlighted in bold.

F_{TA}Ligule~Thickness + C/N (AIC = 56.4)				
Predictor	**Estimate**	**SE**	**t value**	**Pr(>|t|)**
(Intercept)	2.156	2.160	0.998	0.331
Width	−0.032	0.331	−0.097	0.924
Thickness	10.420	2.516	4.141	<0.001 ***
Length	0.003	0.026	0.108	0.915
Fibre	−0.009	0.041	−0.232	0.819
CN	−0.142	0.151	−0.938	0.360
F_{TA}Blade~Thickness + Length (AIC = 62.2)				
Predictor	**Estimate**	**SE**	**t value**	**Pr(>|t|)**
(Intercept)	−0.227	2.401	−0.095	0.926
Width	0.102	0.368	0.279	0.783
Thickness	16.406	2.798	5.864	<0.001 ***
Length	0.017	0.029	0.567	0.578
Fibre	−0.022	0.046	−0.488	0.631
CN	−0.032	0.168	−0.188	0.853

Table 4. *Cont.*

F_{TS}Ligule~Width + C/N (AIC = 49.4)				
Predictor	**Estimate**	**SE**	**t value**	**Pr(>|t|)**
(Intercept)	8.541	1.804	4.734	<0.001 ***
Width	−0.655	0.276	−2.370	0.029 *
Thickness	−2.163	2.102	−1.029	0.316
Length	0.004	0.022	0.183	0.857
Fibre	0.010	0.034	0.302	0.766
CN	−0.221	0.126	−1.749	0.096
F_{TS}Blade~Width + Length + Fibre (AIC = 12.5)				
Predictor	**Estimate**	**SE**	**t value**	**Pr(>|t|)**
(Intercept)	3.242	0.850	3.814	0.001 **
Width	−0.893	0.130	−6.866	<0.001 ***
Thickness	0.080	0.990	0.081	0.936
Length	0.023	0.010	2.222	0.039 *
Fibre	0.037	0.016	2.296	0.033 *
CN	−0.046	0.060	−0.775	0.448

Symbols indicate significant differences at $\alpha < 0.05$ (*); $\alpha < 0.01$ (**); $\alpha < 0.001$ (***).

3.4. Estimated Failure Velocities

A direct relationship was found between the estimated failure velocities and categorical sorting of hydrodynamic locations, with higher velocities required to split the leaf at the ligule in exposed areas (i.e., CH, 19.3 ± 3.6 ms^{-1}) and a decreasing velocity required toward more sheltered locations (i.e., CC, 8.6 ± 1.5 ms^{-1}; Figure 7A). A clear seasonal trend was recorded with higher estimated failure velocities in winter (about 16.8 ± 3.1 ms^{-1}) and minimum velocities required to split the leaf at the ligule in autumn (6.5 ± 1.2 ms^{-1}; Figure 7B).

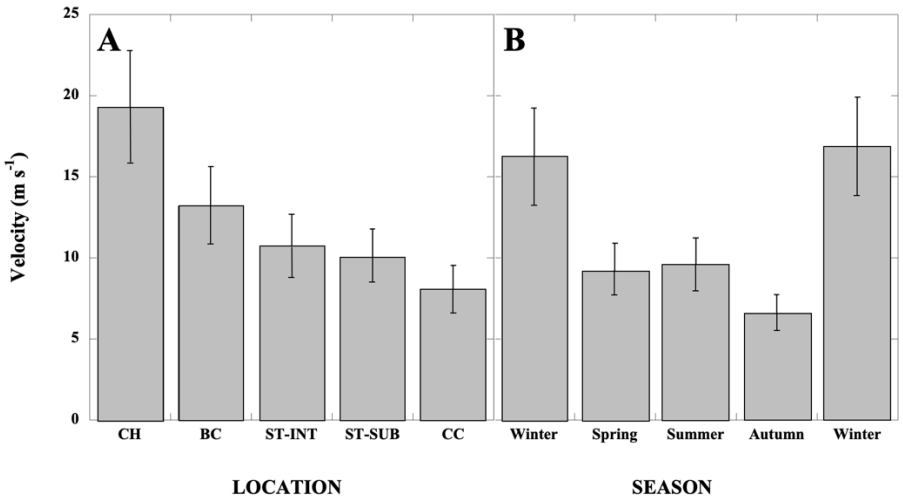

Figure 7. Estimated failure velocities in *Cymodocea nodosa* leaves at the ligule in different locations (**A**) and seasons (**B**). Values are presented as the mean ± SE (n = 4). Locations (from high to low exposure): CH, El Chato (high exposure to waves, intertidal); BC, Bajo de la Cabezuela (medium exposure to waves and currents, subtidal); ST, Santibáñez (low exposure to waves and currents) with two stations: intertidal (ST-Int) and subtidal (ST-Sub); CC, Caño de Cortadura (no waves, low exposure to currents).

4. Discussion

Cymodocea nodosa has evolved a set of adaptations to withstand the large drag forces induced by seawater movement in marine habitats including reduced exposed leaf areas, flexible leaves and, as demonstrated in this study, a weakened point of breakdown in the leaf (i.e., ligule). This singular mechanical design promotes the fracture of the leaf at this point of junction and may reduce the chance of plant uprooting when hydrodynamic forces are extreme. A few studies that have delved into spatial and temporal acclimatization to hydrodynamic conditions concluded that leaf plasticity in morphological and biomechanical traits was the main factor responsible for such acclimatization, while changes in material properties had only a minor influence [11,73]. This study fully agrees with these previous findings, as significant large spatial and temporal differences were found in morphological (i.e., leaf length, width and thickness, surface and cross-sectional areas) and biomechanical (absolute and specific force-to-tear) traits. Moreover, absolute biomechanical traits were highly positively correlated with the cross-sectional area in our study, which indicates that acclimatization to hydrodynamic forces was mainly done by attuning the distribution of the leaf material (i.e., width and thickness of the leaves) without changing the specific material properties. Variation in the intrinsic mechanical properties of the material may reflect underlying variations in cellular structures, possibly via cell orientation, changing anatomy, strengthening of cell wall materials or by increasing the presence of fibres [85,86]. In our study, the low seasonal variation in the leaf fibre content and the large reduction recorded in the content from autumn to winter may clearly indicate that the leaf fibre content played only a residual role in the reinforcement of the blade during winter. Since increasing the fibre content to strengthen and toughen the leaves may require carbon-based resources, a trade-off may exist in resource investment into growth under these season's conditions. Further, low light levels and low temperatures may substantially reduce the gain in the carbon balance of the plants [10]. Additionally, it should be considered that, within each location, the morphological acclimatization to seasonal abiotic variability (e.g., light levels, temperature, nutrients, etc.) is primarily accomplished by a counterbalance between carbon (i.e., light capture) and nutrient requirements [87–91]. However, in the case of whole-leaf mechanical properties such as the absolute force-to-tear (F_{TA}), this is likely a by-product of acclimation to these main environmental factors since F_{TA} depended on the cross-sectional area and intrinsic material properties ([11,73,80] and this study). Regardless, it is interesting to analyse the differential responses of the three studied subtidal populations from this work regarding their own hydrodynamic conditions: the BC populations, although subtidal, were subjected to strong currents, and therefore an extreme trade-off between light capture and drag force reduction is expected. Since the plant surface area is related directly to light capture and inversely to drag forces, plants from this location have to maximize their surface area but also need to be very strong [11,73,92–95]. The plant surface area had intermediate values, while the highest F_{TA} values were recorded at this location. In this case, this high value of F_{TA} was mainly accomplished by leaf reinforcement (i.e., highest values of F_{TS}) and by leaf thickening. Although this response may imply higher construction costs and an increase in the flexural stiffness [11,12,86,96], this study demonstrated that this response allowed plants to resist strong currents before leaf failure.

In addition, although this species faces spatial and temporal changes in hydrodynamic forces by acclimatizing at both morphological and biomechanical levels, the force required to rip the leaf at the ligule followed a seasonal trend, reaching minimum values in autumn at all locations, and coinciding with the lowest estimated velocities for leaf failure. Whether this seasonal weakness at the ligule level can be ascribed to seasonal senescence or to plant acclimation to seasonal abiotic (e.g., light, temperature, nutrients, hydrodynamics, among others) and biotic (e.g., canopy properties) conditions is still uncertain, and further research is needed. To resist and survive hydrodynamic conditions, seagrasses have converged on a morphology based on flexible, narrow, unbranched leaves with a reduced exposed area, reducing the drag forces [80,97,98]. Our study is in agreement with these claims, as *C. nodosa* is greatly flexible [28,73] and has a low exposed area irrespective of season and

location ([75] and this study). However, this study constitutes a step beyond because our results demonstrated that the breaking force was repeatedly higher at the blade than at the ligule, and therefore leaf dislodgement mainly took place at this point of junction. This was also clearly indicated by the breaking pattern found in this species when subjecting the whole leaf to the mechanical assays, as the whole leaf ripped continuously at the ligule (>95% of the assays). An insignificant percentage (<5%) broke at other parts of the leaf but was mainly associated with experimental faults (e.g., they broke at the grip level or the leaf slipped during the test). This has important ecological consequences for seagrasses. For instance, most seagrass species have leaves with a strap-like morphology arising from rhizomes that reconfigure when facing hydrodynamics [12,76,98]. Leaves are clustered in shoots with older leaves allocated in the outermost part of the shoots, while younger ones, and meristems of growth, are in the inner part of the shoot protected by the oldest sheath [99,100]. The oldest leaves are often the longest ones [27,76,101] and also usually bear the highest proportion of epiphytic organisms [102], which may increase the drag experienced by the whole plant. Moreover, some studies have demonstrated that during the ontogenetic development of the shoots, leaves become significantly weaker as they age [39,103]. Therefore, an unexpected sharp increase in hydrodynamic forces may produce an extreme drag over the whole plant, increasing the probability of plant dislodgement. This potential threat can be evolutionarily highly reduced by sacrificing the oldest leaves, as the force needed to dislodge the leaf is regularly lower at the ligule, by at least one-half, than at the blade ([39], this study). Thus, this biomechanical design may promote the premature leaf abscission of the oldest leaf, and therefore it can be an adaptive strategy to reduce sudden and acute drag forces experienced by plants to lessen the chance of whole-plant uprooting. A similar expectation exists in terrestrial plants in storm-exposed areas, as the loss of foliage and branch shedding may reduce the drag and the potential for stem breakage and uprooting [104–106].

In this temperate seagrass, both absolute and specific forces to tear at the ligule level showed a seasonal trend in most locations (with the exception of CC, with very low hydrodynamics and no waves, [107]), which indicates a weakening of this junction towards autumn, suggesting that seasonal senescence may be acting in *C. nodosa*, similar to terrestrial plants, where a shorter photoperiod and cooler temperatures trigger leaf abscission in autumn [108]. However, as aforementioned, individual seagrass plants respond to seasonal abiotic (e.g., light levels, nutrient concentration, temperature, etc.) and biotic (e.g., shoot density, macroalgae and epiphyte coverage, etc.) conditions by progressively altering their morphology, internal composition and biomechanical traits [38,73,109]. While most of these aforementioned abiotic factors follow progressive trends without acute sudden changes or variability at short time scales (e.g., cloud presence, rainfall runoff, heat waves, etc.), acute and sudden changes in hydrodynamic forces are frequently produced in coastal areas. As a consequence, devasting effects on seagrass plants and populations are produced. For instance, our results showed that *C. nodosa* plants in summer–autumn had the highest plant surface area at all locations, while absolute and specific breaking forces at the ligule (i.e., F_{TA} and F_{TS}) reached minimum values at all locations in autumn. Moreover, the F_{TA} Blade/F_{TA} ligule ratio was significantly higher in autumn (about 203%), indicating that a doubling of the force required to break the leaf at the blade was needed in comparison to that at the ligule. Regional and European databases show that storm frequency and intensity follow a seasonal trend with higher values in winter, decreasing to minimum values in summer, with an abrupt increase in autumn [65,110]. Therefore, this sudden and sharp increase in hydrodynamic forces promoted by an increase in storm frequency and intensity may be critical in autumn, as the lowest values for failure velocity were also estimated in this period. Maximum shedding rates usually occur during autumn, suggested by the usual recorded reduction in above-ground biomass in seasonal studies [73,85,88,111–117] and the reported accumulation of nearshore drifting seagrass litter of senescent green leaves worldwide [58–63,118–120]. Consequently, abrupt leaf shedding causes a sudden cessation of the reclamation of leaf nutrient by plants, as the mobilization and removal of substances

from senescing plant tissues and the subsequent transport of these substances to surviving tissues is a highly regulated process [17–21]. In terrestrial plants, abrupt shedding of leaves has also been recorded after the passage of hurricanes, typhoons or even after strong winds. Under such conditions, plants are not able to withdraw nutrients from senescing leaves, and abscised leaves still have a high concentration of nutrients [121–125]. Therefore, the limited rates of nutrient recycling from detached leaves recorded in seagrasses [36,47–51], which bring forward the "nutrient paradox" theory, may be a result of the abrupt interruption of the senescence process because of the sudden autumn increase in hydrodynamic forces that promote the earlier shedding of leaves in the autumn season.

5. Conclusions

This work unraveled the response of the temperate seagrass *Cymodocea nodosa* to a hydrodynamic gradient of exposure on a seasonal basis to explore if leaf fall is due to seasonal senescence or local hydrodynamic conditions. Both absolute and specific forces to tear at the ligule level showed a seasonal trend at most locations, which indicates a weakening of this junction towards autumn. Moreover, the minimum estimated velocities for leaf failure were also recorded in autumn, which may cause the premature shedding of leaves in this season. Therefore, although seasonal senescence may operate in this species, the intensification of storm frequency and, consequently, the increase in hydrodynamic stress in autumn, could favor leaf fall before the senescence process will be completed and all nutrients will be reclaimed by the plant. Key issues still need to be elucidated, including cellular-level molecular analysis of senescence-associated cell death or the nature and control of leaf age [23].

Author Contributions: Conceptualization, R.J.-R., L.G.E., J.J.V. and F.G.B. Methodology: R.J.-R., C.H., L.G.E., J.J.V. and F.G.B., Software: R.J.-R., L.G.E. and F.G.B.; Formal Analyses: R.J.-R., C.H., L.G.E., J.J.V. and F.G.B.; Data curation: R.J.-R., L.G.E. and F.G.B.; Writing—Original Draft Preparation: R.J.-R. and F.G.B.; Writing—Review & Editing: R.J.-R., C.H., L.G.E., J.J.V. and F.G.B.; Funding Acquisition: J.J.V. and F.G.B. All authors have read and agreed to the published version of the manuscript.

Funding: This work was supported by the Spanish Ministry of Economy, Industry and Competitiveness research project PAVAROTTI—[CTM2017-85365-R]. R Jiménez-Ramos and LG Egea hold postdoctoral contracts from the PAVAROTTI project at Universidad de Cádiz (Cádiz, Spain). We thank three anonymous referees for their constructive comments on an earlier version of the manuscript.

Institutional Review Board Statement: Not applicable.

Informed Consent Statement: Not applicable.

Data Availability Statement: The data presented in this study will be available on request.

Acknowledgments: The authors are very grateful to the associate editor and the anonymous reviewers for their valuable comments during the review process.

Conflicts of Interest: The authors declare no conflict of interest.

References

1. Den Hartog, C. *The Sea-Grasses of the World*; North-Holland Publishing Co.: Amsterdam, The Netherlands, 1970; 275p.
2. Arber, A. *Waterplants: A Study of Aquatic Angiosperms*; Cambridge University Press: Cambridge, UK, 1920; p. 436.
3. Olsen, J.L.; Rouzé, P.; Verhelst, B.; Lin, Y.C.; Bayer, T.; Collen, J.; Michel, G. The genome of the seagrass Zostera marina reveals angiosperm adaptation to the sea. *Nature* **2016**, *530*, 331–335. [CrossRef] [PubMed]
4. Hemminga, M.A.; Duarte, C.M. *Seagrass Ecology*; Cambridge University Press: Cambridge, UK, 2000; 289p.
5. Schanz, A.; Asmus, H. Impact of hydrodynamics on development and morphology of intertidal seagrasses in the Wadden Sea. *Mar. Ecol. Prog. Ser.* **2003**, *261*, 123–134. [CrossRef]
6. Read, J.; Stokes, A. Plant biomechanics in an ecological context. *Am. J. Bot.* **2006**, *93*, 1546–1565. [CrossRef]
7. Villazán, B.; Brun, F.G.; González-Ortiz, V.; Moreno-Marín, F.; Bouma, T.J.; Vergara, J.J. Flow velocity and light level drive non-linear response of seagrass Zostera noltei to ammonium enrichment. *Mar. Ecol. Prog. Ser.* **2016**, *545*, 109–121. [CrossRef]
8. Peralta, G.; Brun, F.G.; Pérez-Lloréns, J.L.; Bouma, T.J. Direct effects of current velocity on the growth, morphometry and architecture of seagrasses: A case study on Zostera noltii. *Mar. Ecol. Prog. Ser.* **2006**, *327*, 135–142. [CrossRef]

9. Touchette, B.W. Seagrass-salinity interactions: Physiological mechanisms used by submersed marine angiosperms for a life at sea. *J. Exp. Mar. Biol. Ecol.* **2007**, *350*, 194–215. [CrossRef]
10. De los Santos, C.B.; Onoda, Y.; Vergara, J.J.; Pérez-Lloréns, J.L.; Bouma, T.J.; La Nafie, Y.; Cambridge, M.L.; Brun, F.G. A comprehensive analysis of mechanical and morphological traits in temperate and tropical seagrass species. *Mar. Ecol. Prog. Ser.* **2016**, *551*, 81–94. [CrossRef]
11. Bouma, T.J.; De Vries, M.B.; Low, E.; Peralta, G.; Tánczos, I.V.; van de Koppel, J.; Herman, P.M.J. Trade-offs related to ecosystem engineering: A case study on stiffness of emerging macrophytes. *Ecology* **2005**, *86*, 2187–2199. [CrossRef]
12. Koch, E.W.; Ackerman, J.D.; Verduin, J.; van Keulen, M. Fluid dynamics in seagrass ecology: From molecules to ecosystems. In *Seagrasses: Biology, Ecology and Conservation*; Larkum, A.W.D., Orth, R.J., Duarte, C.M., Eds.; Springer: Dordrecht, The Netherlands, 2006; pp. 193–225.
13. Chaffey, N. Physiological anatomy and function of the membranous grass ligule. *New Phytol.* **2000**, *146*, 5–21. [CrossRef]
14. Quirino, B.F.; Noh, Y.S.; Himelblau, E.; Amasino, R.M. Molecular aspects of leaf senescence. *Trends Plant Sci.* **2000**, *5*, 278–282. [CrossRef]
15. Thomas, H. Senescence, ageing and death of the whole plant. *New Phytol.* **2013**, *197*, 696–711. [CrossRef] [PubMed]
16. Woo, H.R.; Kim, H.J.; Lim, P.O.; Nam, H.G. Leaf senescence: Systems and dynamics aspects. *Ann. Rev. Plant Biol.* **2019**, *70*, 347–376. [CrossRef] [PubMed]
17. Thomas, H.; Ougham, H.; Canter, P.; Donnison, I. What stay-green mutants tell us about nitrogen remobilization in leaf senescence. *J. Exp. Bot.* **2002**, *53*, 801–808. [CrossRef] [PubMed]
18. Avila-Ospina, L.; Moison, M.; Yoshimoto, K.; Masclaux-Daubresse, C. Autophagy, plant senescence, and nutrient recycling. *J. Exp. Bot.* **2014**, *65*, 3799–3811. [CrossRef]
19. Diaz-Mendoza, M.; Velasco-Arroyo, B.; Santamaria, M.E.; González-Melendi, P.; Martinez, M.; Diaz, I. Plant senescence and proteolysis: Two processes with one destiny. *Genet. Mol. Biol.* **2016**, *39*, 329–338. [CrossRef]
20. Mayta, M.L.; Hajirezaei, M.R.; Carrillo, N.; Lodeyro, A.F. Leaf Senescence: The chloroplast connection comes of age. *Plants* **2019**, *8*, 495. [CrossRef]
21. Rasool, S.; Mir, B.A.; Rehman, M.U.; Amin, I.; Mir, M.U.R.; Ahmad, S.B. Abiotic stress and plant senescence. In *Senescence Signalling and Control in Plants*; Academic Press: Cambridge, MA, USA, 2019; pp. 15–17.
22. Christ, B.; Hörtensteiner, S. Mechanism and significance of chlorophyll breakdown. *J. Plant Growth Regul.* **2014**, *33*, 4–20. [CrossRef]
23. Lim, P.O.; Kim, H.J.; Gil Nam, H. Leaf senescence. *Annu. Rev. Plant Biol.* **2007**, *58*, 115–136. [CrossRef]
24. Distelfeld, A.; Avni, R.; Fischer, A.M. Senescence, nutrient remobilization, and yield in wheat and barley. *J. Exp. Bot.* **2014**, *65*, 3783–3798. [CrossRef]
25. Jones, O.R.; Scheuerlein, A.; Salguero-Gómez, R.; Camarda, C.G.; Schaible, R.; Casper, B.B.; Quintana-Ascencio, P.F. Diversity of ageing across the tree of life. *Nature* **2014**, *505*, 169–173. [CrossRef]
26. Roach, D.A.; Smith, E.F. Life-history trade-offs and senescence in plants. *Funct. Ecol.* **2020**, *34*, 17–25. [CrossRef]
27. Jibran, R.; Hunter, D.A.; Dijkwel, P.P. Hormonal regulation of leaf senescence through integration of developmental and stress signals. *Plant Mol. Biol.* **2013**, *82*, 547–561. [CrossRef] [PubMed]
28. Sade, N.; del Mar Rubio-Wilhelmi, M.; Umnajkitikorn, K.; Blumwald, E. Stress-induced senescence and plant tolerance to abiotic stress. *J. Exp. Bot.* **2017**, *69*, 845–853. [CrossRef] [PubMed]
29. Jan, S.; Abbas, N.; Ashraf, M.; Ahmad, P. Roles of potential plant hormones and transcription factors in controlling leaf senescence and drought tolerance. *Protoplasma* **2019**, *256*, 313–329. [CrossRef]
30. Aerts, R. Nutrient resorption from senescing leaves of perennials: Are there general patterns? *J. Ecol.* **1996**, *84*, 597–608. [CrossRef]
31. Greenberg, J.T. Programmed cell death: A way of life for plants. *Proc. Natl. Acad. Sci. USA* **1996**, *93*, 12094–12097. [CrossRef]
32. Larkum, A.W.D.; den Hartog, C. Evolution and biogeography of seagrasses. In *Biology of Seagrasses*; Larkum, A.W.D., Mc Comb, A., Shepherd, S.A., Eds.; Elsevier Science Publishers B.V.: Amsterdam, The Netherlands, 1989; pp. 112–156.
33. Thomas, H.; Huang, L.; Young, M.; Ougham, H. Evolution of plant senescence. *BMC Evol. Biol.* **2009**, *9*, 163. [CrossRef]
34. Mateo, M.A.; Cebrián, J.; Dinton, K.; Mutchler, T. Carbon flux in seagrass ecosystems. In *Seagrasses: Biology, Ecology and Conservation*; Larkum, A.W.D., Orth, R.J., Duarte, C.M., Eds.; Springer: Dordrecht, The Netherlands, 2006; pp. 159–192.
35. Romero, J.; Lee, K.S.; Pérez, M.; Mateo, M.A.; Alcoverro, T. Nutrient dynamics in seagrass ecosystems. In *Seagrasses: Biology, Ecology and Conservation*; Larkum, A.W.D., Orth, R.J., Duarte, C.M., Eds.; Springer: Dordrecht, The Netherlands, 2006; pp. 227–254.
36. Cuoplant, G.T.; Duarte, C.M.; Walker, D.I. High metabolic rates in beach cast communities. *Ecosystems* **2007**, *10*, 1341–1350.
37. Macreadie, P.I.; Trevathan-Tacket, S.M.; Baldock, J.A.; Kelleway, J. Converting beach-cast seagrass wracks into biochar: A climate-friendly solution to a coastal problema. *Sci. Tot. Environ.* **2017**, *574*, 90–94. [CrossRef]
38. Kopp, B.S. Effects of Nitrate Fertilization and Shading on Physiological and Biomechanical Properties of Eelgrass (Zostera Marina). Ph.D. Dissertation, University of Rhode Island, South Kingstown, RI, USA, 1999; 187p.
39. Brun, F.G.; Hernández, I.; Vergara, J.J.; Peralta, G.; Pérez-Lloréns, J.L. Assessing the toxicity of ammonium pulses to the survival and growth of Zostera noltii. *Mar. Ecol. Prog. Ser.* **2002**, *225*, 177–187. [CrossRef]
40. Egea, L.G.; Jiménez-Ramos, R.; Vergara, J.J.; Hernández, I.; Brun, F.G. Interactive effect of temperature, acidification and ammonium enrichment on the seagrass Cymodocea nodosa. *Mar. Pollut. Bull.* **2018**, *134*, 14–26. [CrossRef] [PubMed]

41. Egea, L.G.; Jiménez-Ramos, R.; Hernández, I.; Brun, F.G. Differential effects of nutrient enrichment on carbon metabolism and dissolved organic carbon (DOC) fluxes in macrophytic benthic communities. *Mar. Environ. Res.* **2020**, *162*, 105179. [CrossRef] [PubMed]
42. Serrano, O.; Mateo, M.A.; Renom, P. Seasonal response of Posidonia oceanica to light disturbances. *Mar. Ecol. Prog. Ser.* **2011**, *423*, 29–38. [CrossRef]
43. Brun, F.G.; Hernández, I.; Vergara, J.J.; Pérez-Lloréns, J.L. Growth, carbon allocation and proteolytic activity in the seagrass Zostera noltii shaded by Ulva canopies. *Funct. Plant Biol.* **2003**, *30*, 551–560. [CrossRef] [PubMed]
44. Villazán, B.; Pedersen, M.F.; Brun, F.G.; Vergara, J.J. Elevated ammonium concentrations and low light form a dangerous synergy for eelgrass Zostera marina. *Mar. Ecol. Prog. Ser.* **2013**, *493*, 141–154. [CrossRef]
45. Fonseca, M.S.; Koehl, M.A.R. Flow in seagrass canopies: The influence of patch width. *Estuar. Coast. Shelf Sci.* **2006**, *67*, 1–9. [CrossRef]
46. Hemminga, M.A.; Harrison, P.G.; Van Lent, F. The balance of nutrient losses and gains in seagrass meadows. *Mar. Ecol. Prog. Ser.* **1991**, *71*, 85–96. [CrossRef]
47. Pedersen, M.F.; Borum, J. An annual nitrogen budget for a seagrass Zostera marina population. *Mar. Ecol. Prog. Ser.* **1993**, *101*, 169–177. [CrossRef]
48. Mateo, M.A.; Romero, J. Detritus dynamics in the seagrass Posidonia oceanica: Elements for an ecosystem carbon and nutrient Budget. *Mar. Ecol. Prog. Ser.* **1997**, *151*, 43–53. [CrossRef]
49. Stapel, J.; Hemminga, M.A. Nutrient resorption from seagrass leaves. *Mar. Biol.* **1997**, *128*, 197–206. [CrossRef]
50. Hemminga, M.A. The root rhizome system of seagrasses: An asset and a burden. *J. Sea Res.* **1998**, *39*, 183–196. [CrossRef]
51. Hemminga, M.A.; Marbá, N.; Stapel, J. Leaf nutrient resorption, leaf lifespan and the retention of nutrients in seagrass systems. *Aquat. Bot.* **1999**, *65*, 141–158. [CrossRef]
52. Lepoint, G.; Defawe, O.; Gobert, S.; Dauby, P.; Bouquegneau, J.M. Experimental evidence for N recycling in the leaves of the seagrass Posidonia oceanica. *J. Sea Res.* **2002**, *48*, 173–179. [CrossRef]
53. Chapin, F.S., III; Kedrowski, R.A. Seasonal changes in nitrogen and phosphorus fractions and autumn retranslocation in evergreen and deciduous taiga trees. *Ecology* **1983**, *64*, 379–391. [CrossRef]
54. Yuan, Z.Y.; Chen, H.Y. Global-scale patterns of nutrient resorption associated with latitude, temperature and precipitation. *Glob. Ecol. Biogeogr.* **2009**, *18*, 11–18. [CrossRef]
55. Reed, S.C.; Townsend, A.R.; Davidson, E.A.; Cleveland, C.C. Stoichiometric patterns in foliar nutrient resorption across multiple scales. *New Phytol.* **2012**, *196*, 173–180. [CrossRef]
56. Brant, A.N.; Chen, H.Y. Patterns and mechanisms of nutrient resorption in plants. *Crit. Rev. Plant Sci.* **2015**, *34*, 471–486. [CrossRef]
57. Ochieng, C.A.; Erftemeijer, P.L.A. Accumulation of seagrass beach cast along the Kenyan coast: A quantitative assessment. *Aquat. Bot.* **1999**, *65*, 221–238. [CrossRef]
58. Balestri, E.; Vallerini, F.; Lardicci, C. Qualitative and quantitative assessment of the reproductive litter from Posidonia oceanica accumulated on a sand beach following a storm. *Estuar. Coast. Shelf Sci.* **2006**, *66*, 30–34. [CrossRef]
59. Mateo, M.A. Beach-Cast Cymodocea nodosa along the shore of a semienclosed say: Sampling and elements to assess its ecological implications. *J. Coast. Res.* **2010**, *26*, 283–291. [CrossRef]
60. Simeone, S.; De Muro, S.; De Falco, G. Seagrass berm deposition on a Mediterranean embayed beach. *Estuar. Coast. Shelf Sci.* **2013**, *135*, 171–181. [CrossRef]
61. Oldham, C.; McMahon, K.; Brown, E.; Bosserelle, C.; Lavery, P. A preliminary exploration of the physical properties of seagrass wrack that affect its offshore transport, deposition, and retention on a beach. *Limnol. Oceanogr. Fluids Environ.* **2014**, *4*, 120–135. [CrossRef]
62. Prasad, M.H.K.; Ganguly, D.; Paneerselvam, A.; Ramesh, R.; Purvaja, R. Seagrass litter decomposition: An additional nutrient source to shallow coastal waters. *Environ. Monit. Assess.* **2019**, *191*, 5. [CrossRef] [PubMed]
63. Morre, D.J. Cell wall dissolution and enzyme secretion during leaf abscission. *Plant Physiol.* **1968**, *43*, 1545–1559. [PubMed]
64. Anfuso, G.; Rangel-Buitrago, N.; Cortés-Useche, C.; Iglesias-Castillo, B.; Gracia, F.J. Characterization of storm events along the Gulf of Cadiz (eastern central Atlantic Ocean). *Int. J. Climatol.* **2016**, *36*, 3690–3707. [CrossRef]
65. Del Río, L.; Plomaritis, T.A.; Benavente, J.; Valladares, M.; Ribera, P. Establishing storm thresholds for the Spanish Gulf of Cádiz coast. *Geomorphology* **2012**, *143*, 13–23. [CrossRef]
66. Jiménez-Ramos, R.; Egea, L.G.; Vergara, J.J.; Brun, F.G. Factors modulating herbivory patterns in Cymodocea nodosa meadows. *Limnol. Oceanogr.* **2021**, *66*, 2218–2233. [CrossRef]
67. Peralta, G.; Godoy, O.; Egea, L.G.; de los Santos, C.B.; Jiménez-Ramos, R.; Lara, M.; Brun, F.G.; Hernández, I.; Olivé, I.; Vergara, J.J.; et al. The morphometric acclimation to depth explains the long-term resilience of the seagrass Cymodocea nodosa in a shallow tidal lagoon. *J. Environ. Res.* **2021**, *299*, 113452. [CrossRef]
68. Morris, E.P.; Peralta, G.; Van Engeland, T.; Bouma, T.J.; Brun, F.G.; Lara, M.; Lucas Perez-Lloréns, J.L. The role of hydrodynamics in structuring in situ ammonium uptake within a submerged macrophyte community. *Limnol. Oceanogr. Fluids Environ.* **2013**, *3*, 210–224. [CrossRef]
69. Kagan, B.A.; Álvarez, O.; Izquierdo, A.; Mañanes, R.; Tejedor, B.; Tejedor, L. Weak wind-wave/tide interaction over a moveable bottom: Results of numerical experiments in Cádiz Bay. *Cont. Shelf Res.* **2003**, *23*, 435–456. [CrossRef]

70. Lara, M.; Peralta, G.; Alonso, J.J.; Morris, E.P.; González-Ortiz, V.; Rueda-Márquez, J.J.; Pérez-Lloréns, J.J. Effects of intertidal seagrass habitat fragmentation on turbulent diffusion and retention time of solutes. *Mar. Pollut. Bull.* **2012**, *64*, 2471–2479. [CrossRef] [PubMed]
71. Olivé, I.; Vergara, J.J.; Pérez-Lloréns, J.L. Photosynthetic and morphological photoacclimation of the seagrass Cymodocea nodosa to season, depth and leaf position. *Mar. Biol.* **2013**, *160*, 285–297. [CrossRef]
72. Egea, L.G.; Barrón, C.; Jiménez-Ramos, R.; Hernández, I.; Vergara, J.J.; Pérez-Lloréns, J.L.; Brun, F.G. Coupling carbon metabolism and dissolved organic carbon fluxes in benthic and pelagic coastal communities. *Estuar. Coast. Shelf Sci.* **2019**, *227*, 106336. [CrossRef]
73. De los Santos, C.B.; Brun, F.G.; Pérez-lloréns, J.L. New aspect in seagrass acclimation: Leaf mechanical properties vary spatially and seasonally in the temperate species Cymodocea nodosa Ucria (Ascherson). *Mar. Biol.* **2013**, *160*, 1083–1093. [CrossRef]
74. Brun, F.G.; Vergara, J.J.; Hernández, I.; Pérez-Lloréns, J.L. Evidence for vertical growth in Zostera noltii Hornem. *Bot. Mar.* **2005**, *48*, 446–450. [CrossRef]
75. Puertos del Estado. Red Costera de Boyas. Informe de datos de la boya de Cádiz. Periodo: Sept. 2015–2016. Available online: https://www.puertos.es/es-es/oceanografia/ (accessed on 15 February 2018).
76. Kuo, J.; Den Hartog, C. Seagrass morphology, anatomy, and ultrastructure. In *Seagrasses: Biology, Ecology and Conservation*; Larkum, A.W.D., Orth, R.J., Duarte, C.M., Eds.; Springer: Dordrecht, The Netherlands, 2006; pp. 51–87.
77. Van Soest, P.J.; Robertson, J.B.; Lewis, B.A. Methods for dietary fiber, neutral detergent fiber, and non starch polysaccharides in relation to animal nutrition. *J. Dairy Sci.* **1991**, *74*, 3583–3597. [CrossRef]
78. Gere, J.M.; Goodno, B.J. *Mechanics of Materials*; Cengage Learning: Stamford, CT, USA, 2012.
79. Denny, M.W. *Biology and the Mechanics of the Wave-Swept Environment*; Princeton University Press: Princeton, NJ, USA, 1988; 329p.
80. Vogel, S. *Life in Moving Fluids: The Physical Biology of Flow*; Princeton University Press: London, UK, 1994; 467p.
81. Wei, T.; Simko, V. Visualization of a Correlation Matrix. Statistician 2017, 56. Available online: https://github.com/taiyun/corrplot (accessed on 13 September 2019).
82. Harrison, X.A.; Donaldson, L.; Correa-Cano, M.E.; Evans, J.; Fisher, D.N.; Goodwin, C.E.D.; Robinson, B.S.; Hodgson, D.J.; Inger, R. A brief introduction to mixed effects modelling and multi-model inference in ecology. *PeerJ* **2018**, *6*, e4794. [CrossRef]
83. Barton, K. Multi-Model Inference. R package 1.43.15 (Issues 1–34). 2019. Available online: https://CRAN.R-project.org/package=MuMIn (accessed on 10 February 2020).
84. R Core Team. *R: A Language and Environment for Statistical Computing*; R Foundation for Statistical Computing: Vienna, Austria, 2020; Available online: http://www.r-project.org/index.html (accessed on 3 January 2021).
85. Onoda, Y.; Hikosaka, K.; Hirose, T. Allocation of nitrogen to cell walls decreases photosynthetic nitrogen-use efficiency. *Funct. Ecol.* **2004**, *18*, 419–425. [CrossRef]
86. Lamberti-Raverot, B.; Puijalon, S. Nutrient enrichment affects the mechanical resistance of aquatic plants. *J. Exp. Bot.* **2012**, *63*, 6115–6123. [CrossRef]
87. Brun, F.G.; Vergara, J.J.; Peralta, G.; García-Sánchez, M.P.; Hernández, I.; Pérez-Lloréns, J.L. Clonal building, simple growth rules and phylloclimate as key steps to develop functional-structural seagrass models. *Mar. Ecol. Prog. Ser.* **2006**, *323*, 133–148. [CrossRef]
88. Lee, K.-S.; Park, S.R.; Kim, Y.K. Effects of irradiance, temperature, and nutrients on growth dynamics of seagrasses: A review. *J. Exp. Mar. Biol. Ecol.* **2007**, *350*, 144–175. [CrossRef]
89. Ferguson, A.J.; Gruber, R.K.; Orr, M.; Scanes, P. Morphological plasticity in Zostera muelleri across light, sediment, and nutrient gradients in Australian temperate coastal lakes. *Mar. Ecol. Prog. Ser.* **2016**, *556*, 91–104. [CrossRef]
90. Enríquez, S.; Olivé, I.; Cayabyab, N.; Hedley, J.D. Structural complexity governs seagrass acclimatization to depth with relevant consequences for meadow production, macrophyte diversity and habitat carbon storage capacity. *Sci. Rep.* **2019**, *9*, 1–14. [CrossRef] [PubMed]
91. Duarte, C.M. Seagrass depth limits. *Aquat. Bot.* **1991**, *40*, 363–377. [CrossRef]
92. Onoda, Y.; Westoby, M.; Adler, P.B.; Choong, A.M.F.; Clissold, F.J.; Cornelissen, J.H.; Díaz, S.; Dominy, N.J.; Elgart, A.; Enrico, L.; et al. Global patterns of leaf mechanical properties. *Ecol. Lett.* **2011**, *14*, 301–312. [CrossRef] [PubMed]
93. Zimmerman, R.C. Light and photosynthesis in seagrass meadows. In *Seagrasses: Biology, Ecology and Conservation*; Larkum, A.W.D., Orth, R.J., Duarte, C.M., Eds.; Springer: Dordrecht, The Netherlands, 2006; pp. 303–321.
94. Alcoverro, T.; Duarte, C.M.; Romero, J. Annual growth dynamics of Posidonia oceanica: Contribution of large-scale versus local factors to seasonality. *Mar. Ecol. Prog. Ser.* **1995**, *120*, 203–210. [CrossRef]
95. Koch, E.W. Hydrodynamics, diffusion-boundary layers and photosynthesis of the seagrasses Thalassia testudinum and Cymodocea nodosa. *Mar. Biol.* **1994**, *118*, 767–776. [CrossRef]
96. Bouma, T.J.; Friedrichs, M.; Klaassen, P.; Van Wesenbeeck, B.K.; Brun, F.G.; Temmerman, S.; Herman, P.M.J. Effects of shoot stiffness, shoot size and current velocity on scouring sediment from around seedlings and propagules. *Mar. Ecol. Prog. Ser.* **2009**, *388*, 293–297. [CrossRef]
97. Fonseca, M.S.; Koehl, M.A.R.; Fourqurean, J.W. Effect of seagrass on current speed: Importance of flexibility versus shoot density. *Front. Mar. Sci.* **2019**, *6*, 376. [CrossRef]
98. Paul, M.; de los Santos, C.B. Variation in flexural, morphological, and biochemical leaf properties of eelgrass (Zostera marina) along the European Atlantic climate regions. *Mar. Biol.* **2019**, *166*, 127. [CrossRef]

99. Brun, F.G.; Perez-Pastor, A.; Hernández, I.; Vergara, J.J.; Pérez-Lloréns, J.L. Shoot organization in the seagrass Zostera noltii: Implications for space occupation and plant architecture. *Helgol. Mar. Res.* **2006**, *60*, 59–69. [CrossRef]
100. Jacobs, R.P.W.M. Distribution and aspects of the production and biomass of eelgrass, *Zostera marina* L., at Roscoff, France. *Aquat. Bot.* **1979**, *7*, 151–172. [CrossRef]
101. De los Santos, C.B.; Vicencio-Rammsy, B.; Lepoint, G.; Remy, F.; Bouma, T.J.; Gobert, S. Ontogenic variation and effect of collection procedure on leaf biomechanical properties of Mediterranean seagrass *Posidonia oceanica* (L.) Delile. *Mar. Ecol.* **2016**, *37*, 750–759. [CrossRef]
102. Schönemann, A.M. Estimations of the Net Primary Production of Epiphytes in Seagrass Populations from Cádiz Bay. Master's Thesis, University of Cádiz, Cádiz, Spain, 2015; 40p.
103. Hedden, R.L.; Fredericksen, T.S.; Williams, S.A. Modeling the effect of crown shedding and streamlining on the survival of loblolly pine exposed to acute wind. *Can. J. For. Res.* **1995**, *25*, 704–712. [CrossRef]
104. Vollsinger, S.; Mitchell, S.J.; Byrne, K.E.; Novak, M.D.; Rudnicki, M. Wind tunnel measurements of crown streamlining and drag relationships for several hardwood species. *Can. J. For. Res.* **2005**, *35*, 1238–1249. [CrossRef]
105. Mitchell, S.J. Wind as a natural disturbance agent in forests: A synthesis. *Forestry* **2013**, *86*, 147–157. [CrossRef]
106. Lee, Y.; Yoon, T.H.; Lee, J.; Jeon, S.Y.; Lee, J.H.; Lee, M.K.; Cho, H.K. A lignin molecular brace controls precision processing of cell walls critical for surface integrity in Arabidopsis. *Cell* **2018**, *173*, 1468–1480. [CrossRef]
107. De los Santos, C.B.; Godbold, J.A.; Solan, M. Short-term growth and biomechanical responses of the temperate seagrass Cymodocea nodosa to CO2 enrichment. *Mar. Ecol. Prog. Ser.* **2017**, *572*, 91–102. [CrossRef]
108. Patharkar, O.R.; Walker, J.C. Advances in abscission signaling. *J. Exp. Bot.* **2018**, *69*, 733–740. [CrossRef]
109. La Nafie, Y.; de los Santos, C.B.; Brun, F.G.; van Katwijk, M.; Bouma, T.J. Waves and high nutrient loads jointly decrease survival and separately affect morphological and biomechanical properties in the seagrass Zostera noltii. *Limnol. Oceanogr.* **2012**, *57*, 1667–1672. [CrossRef]
110. Molina, R.; Manno, G.; Lo Re, C.; Anfuso, G.; Ciraolo, G. Storm Energy Flux Characterization along the Mediterranean Coast of Andalusia (Spain). *Water* **2019**, *11*, 509. [CrossRef]
111. Vermaat, J.E.; Hootsmans, M.J.M.; Nienhuis, P.H. Seasonal dynamics and leaf growth of Zostera noltii Hornem., a perennial intertidal seagrass. *Aquat. Bot.* **1987**, *28*, 287–299. [CrossRef]
112. Kerr, E.A.; Strother, S. Seasonal changes in standing crop of Zostera muelleri in south-eastern Australia. *Aquat. Bot.* **1990**, *38*, 369–376. [CrossRef]
113. Romero, J.; Pergent, G.; Pergent-Martini, C.; Mateo, M.A.; Regnier, C. The detritic compartment in a Posidonia oceanica meadow: Litter features, decomposition rates, and mineral stocks. *Mar. Ecol.* **1992**, *13*, 69–83. [CrossRef]
114. Kraemer, G.P.; Mazzella, L. Nitrogen acquisition, storage, and use by the Mediterranean seagrasses Cymodocea nodosa and Zostera noltii. *Mar. Ecol. Prog. Ser.* **1999**, *183*, 95–103. [CrossRef]
115. Guidetti, P.; Lorenti, M.; Buia, M.C.; Mazzella, L. Temporal Dynamics and Biomass Partitioning in Three Adriatic Seagrass Species: Posidonia oceanica, Cymodocea nodosa, Zostera marina. *Mar. Ecol.* **2002**, *23*, 51–67. [CrossRef]
116. Orth, R.J.; Moore, K.A.; Marion, S.R.; Wilcox, D.J.; Parrish, D.B. Seed addition facilitates eelgrass recovery in a coastal bay system. *Mar. Ecol. Prog. Ser.* **2012**, *448*, 177–195. [CrossRef]
117. Newell, S.Y.; Fell, J.W.; Statzell-Tallman, A.; Miller, C.; Cefalu, R. Carbon and nitrogen dynamics in decomposing leaves of three coastal marine vascular plants of the subtropics. *Aquat. Bot.* **1984**, *19*, 183–192. [CrossRef]
118. Kirkman, H.; Kendrick, G.A. Ecological significance and commercial harvesting of drifting and beach-cast macro-algae and seagrasses in Australia: A review. *J. Appl. Phycol.* **1997**, *9*, 311. [CrossRef]
119. Colombini, I.; Chelazzi, L.; Gibson, R.N.; Atkinson, R.J.A. Influence of marine allochthonous input on sandy beach communities. *Oceanogr. Mar. Biol. Annu. Rev.* **2003**, *41*, 115–159.
120. Portillo, E. Relation between the type of wave exposure and seagrass losses (*Cymodocea nodosa*) in the south of Gran Canaria (Canary Islands—Spain). *Oceanol. Hydrobiol. Stud.* **2014**, *43*, 29–40. [CrossRef]
121. Dewit, L.; Reid, D.M. Branch abscission in balsam poplar (Populus balsamifera): Characterization of the phenomenon and the influence of wind. *Int. J. Plant Sci.* **1992**, *153*, 556–564. [CrossRef]
122. Rybczyk, J.M.; Zhang, X.W.; Day, J.W., Jr.; Hesse, I.; Feagley, S. The impact of Hurricane Andrew on tree mortality, litterfall, nutrient flux, and water quality in a Louisiana coastal swamp forest. *J. Coast. Res.* **1995**, *21*, 340–353.
123. Inagaki, Y.; Sakai, A.; Kuramoto, S.; Kodani, E.; Yamada, T.; Kawasaki, T. Inter-annual variations of leaf-fall phenology and leaf-litter nitrogen concentration in a hinoki cypress (Chamaecyparis obtusa Endlicher) stand. *Ecol. Res.* **2008**, *23*, 965–972. [CrossRef]
124. Lugo, A.E. Visible and invisible effects of hurricanes on forest ecosystems: An international review. *Austral Ecol.* **2008**, *33*, 368–398. [CrossRef]
125. Telewski, F.W. Is windswept tree growth negative thigmotropism? *Plant Sci.* **2012**, *184*, 20–28. [CrossRef]